Vector mesons

1972 J. Phys. A: Gen. Phys. 5 327

(http://iopscience.iop.org/0022-3689/5/3/003)

J. Phys. A: Gen. Phys., Vol. 5, March 1972. Printed in Great Britain

Vector mesons†

E GABATHULER

Daresbury Nuclear Physics Laboratory, Daresbury, Cheshire, UK

MS received 20 October 1971

Abstract. Vector mesons with the same quantum numbers as the photon are expected to play an important role in electromagnetic interactions. The study of the electromagnetic decays of these mesons and their production by photons has provided related information which can be used to understand this interaction. The experimental information which is currently available is presented and compared with existing theoretical ideas in this article.

1. Introduction

The vector mesons with the quantum numbers of the photon ($J^{PC} = 1^{--}$) have provided us with a very large field of interesting physics since their existence was first predicted by Nambu (1957) from elastic electron–proton scattering. In the SU(3) classification scheme for 1^- mesons, the ρ is a triplet state and the ω and ϕ mesons arise due to mixing of pure singlet and octet states. The determination of the photon–vector meson coupling strengths ($em_v^2/2\gamma_v$) and the amount of ω–ϕ mixing has led to a large number of experiments on vector meson production at proton and electron accelerators since these mesons were first observed in 1961–2. The introduction of electron–positron storage rings has given us a new and powerful method of studying these vector mesons.

2. Determination of γ_v

There are two methods of obtaining a direct measurement of the γ–v coupling as illustrated in figure 1. In the first method, the electron and positron annihilate to produce a vector meson in the final state via an intermediate time-like photon. In the second method, the vector mesons are produced in a hadronic interaction and subsequently decay into a time-like photon. The colliding beam method is simpler than the hadronic production, where the electron pairs have to be measured in a large background of other particles.

The simplicity of the colliding beam experiment is illustrated in figure 2, which shows the apparatus used by an Orsay group (Augustin *et al* 1969a), consisting of simple spark chamber arrays above and below the intersecting beam region. The energy determination is obtained from the electron and positron in the initial state and the particle identification is obtained by range and coplanarity measurements. The power of the storage ring as a device of very precise energy resolution is illustrated in figure 3, where the excitation curve shows a clearly resolved peak at the mass of the ϕ meson, which has a full width at half maximum (FWHM) of about 4 MeV.

† Review talk given at the Lancaster Conference of the Institute of Physics, April, 1971.

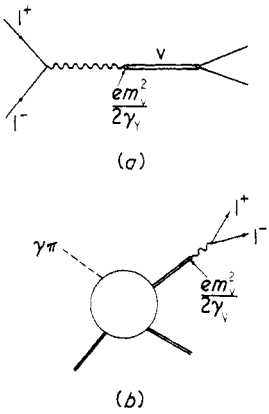

Figure 1. Two methods of obtaining directly the γ–v coupling strengths. (*a*) Colliding beams $(e^+ + e^- \to v)$, $\sigma_{ER}(e^+ + e^- \to v) = (12\pi/m_v^2)\Gamma(v \to e^+e^-)/\Gamma(v \to \text{all})$; (*b*) hadronic production $(v \to e^+e^-)$, $BR = \Gamma(v \to e^+e^-)/\Gamma(v \to \text{all}) = \frac{1}{12}\alpha^2(\gamma_v^2/4\pi)^{-1}(m_v/\Gamma(v))\{1 - \phi(m_e/m_v)\}^2$.

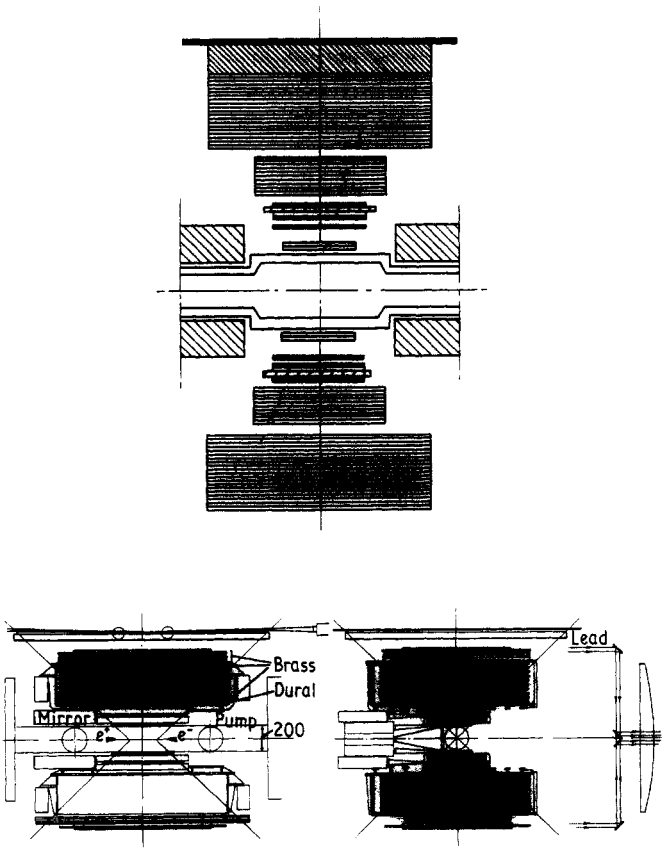

Figure 2. Orsay detection apparatus, for measuring ρ, ω and ϕ meson production, consisting of thin plate and thick plate spark chambers (see Augustin *et al* 1969a).

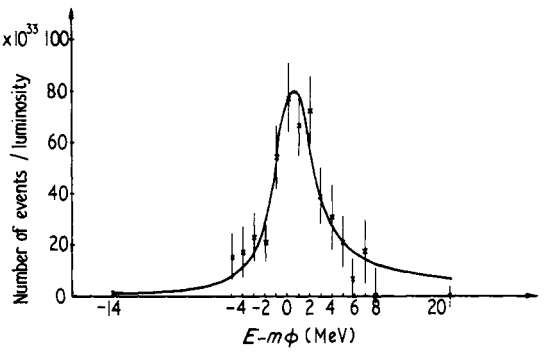

Figure 3. The Orsay excitation curve in the region of the ϕ meson measured in 1 MeV intervals.

The results of the various experiments are presented in table 1, and show that for the different methods, the results are in reasonable agreement. The results for the ω meson in hadronic production should be treated with caution due to final state interference effects. This will be discussed in more detail later.

Table 1. Determinations of leptonic branching ratios of the vector mesons

	$B_\rho \times 10^5$	$B_\omega \times 10^5$	$B_\phi \times 10^5$
Bologna–CERN ($\pi P \to V$)	—	$4{\cdot}0 \pm 1{\cdot}5$	$6{\cdot}1 \pm 2{\cdot}6$
CERN ($\pi P \to V$)	$9{\cdot}7^{+2{\cdot}0}_{-2{\cdot}3}$	—	—
Cornell ($\gamma P \to V$)	$5{\cdot}3 \pm 1{\cdot}5$	—	$1{\cdot}9 \pm 0{\cdot}6$
Daresbury ($\gamma P \to V$)	$4{\cdot}9^{+1{\cdot}2}_{-1{\cdot}5}$	$7{\cdot}8 \pm 2{\cdot}7$	—
Dubna ($\pi P \to V$)	$5{\cdot}3 \pm 1{\cdot}1$	—	$6{\cdot}6 \pm 4{\cdot}4$
Harvard–AGS ($\pi P \to V$)	$5{\cdot}6 \pm 1{\cdot}1$	—	$3{\cdot}5^{+3{\cdot}5}_{-1{\cdot}7}$
MIT–DESY ($\gamma P \to V$)	$6{\cdot}5 \pm 1{\cdot}4$	—	$3{\cdot}6 \pm 0{\cdot}9$
North Eastern–CEA ($\gamma P \to V$)	$7{\cdot}9 \pm 2{\cdot}0$	—	$2{\cdot}2 \pm 0{\cdot}6$
Novosibirsk (colliding beam)	$5{\cdot}0 \pm 1{\cdot}0$	—	$2{\cdot}81 \pm 0{\cdot}25$
Orsay (colliding beam)	$6{\cdot}63 \pm 0{\cdot}85$	$7{\cdot}8 \pm 1{\cdot}4$	$3{\cdot}45 \pm 0{\cdot}27$
Rutherford Imperial College ($\pi P \to V$)	—	$20{\cdot}0 \pm 12{\cdot}0$	$7{\cdot}2 \pm 3{\cdot}9$

The mixing angles and coupling constants determined from the complete set of Orsay results are presented in table 2 and show that the time-like photon couples approximately seven times more strongly to the ρ meson than either the ω or ϕ mesons. However, in order to distinguish between the various mixing models, more precise data, particularly for the ω meson, are required.

If we assume that γ_v is independent of whether the photon is real or time-like, then we might expect on simple arguments that real photons would produce vector mesons by a diffractive mechanism in the same ratios as those given by colliding beam results. Vector meson photoproduction has provided answers to some of these assumptions, but as we shall see there are many problems to be resolved in this field.

Table 2. Mixing angle and coupling constants with finite width factor (Orsay results)

$\left(\frac{\gamma_\rho^2}{4\pi}\right)^{-1} = 1{\cdot}99 \pm 0{\cdot}19$ $\left(\frac{\gamma_\omega^2}{4\pi}\right)^{-1} = 14{\cdot}0 \pm 2{\cdot}8$ $\left(\frac{\gamma_\phi^2}{4\pi}\right)^{-1} = 11{\cdot}0 \pm 0{\cdot}9$

$\left(\frac{\gamma_S^2}{4\pi}\right)^{-1} = 1{\cdot}55 \pm 0{\cdot}15$

$\theta_V = (41{\cdot}5 \pm 3)^\circ$ $\theta_N = (13{\cdot}5 \pm 2)^\circ$ $\theta = (23{\cdot}1 \pm 4)^\circ$

If the factor K is chosen to get the conventional normalization to 9 or the ρ inverse coupling:

$K\left(\frac{\gamma_\rho^2}{4\pi}\right)^{-1} = 9$ $K\left(\frac{\gamma_\omega^2}{4\pi}\right)^{-1} = 1{\cdot}28 \pm 0{\cdot}28$ $K\left(\frac{\gamma_\phi^2}{4\pi}\right)^{-1} = 1{\cdot}63 \pm 0{\cdot}20$

Theory	Predictions		
	$K(\gamma_\rho^2/4\pi)^{-1}$	$K(\gamma_\omega^2/4\pi)^{-1}$	$K(\gamma_\phi^2/4\pi)^{-1}$
SU6	9	1	2
Current mixing	9	0·79	1·89
Mass mixing	9	0·72	1·11

3. Photoproduction of vector mesons

The production of vector mesons by photons has turned out to be a very interesting field of study for the following reasons:

(i) The production of ρ, ω and φ mesons by a particle of the same quantum numbers can proceed by pomeron exchange and this provides a unique source of vector mesons by diffractive production off nuclei.
(ii) The decay of spin 1 mesons provides information on the production mechanism.
(iii) Information on the photon–vector-pseudoscalar meson (γvP) couplings can be obtained from t channel exchange amplitudes.
(iv) The use of linear polarized photons produced by coherent scattering off diamond crystals or backward Compton scattering by polarized laser beams separates out natural and unnatural parity t channel exchange contributions.
(v) Polarized photons and meson decay angular distributions provide information similar to that using polarized targets and recoil nucleon polarization measurements in pion–nucleon scattering, for example, R and A parameters.

Photoproduction of vector mesons can be simply described by the vector dominance model, which can be expressed as

$$\gamma_\mu^{\text{em}}(x) = -\sum \frac{m_\rho^2}{2\gamma_\mu}\rho_\mu^0(x) + \frac{m_\omega^2}{2\gamma_\rho}\omega_\mu(x) + \frac{m_\phi^2}{2\gamma_\phi}\phi_\mu(x) + \ldots$$

$$= -\sum \frac{m_v^2}{2\gamma_v} V_\mu(x)$$

where $\gamma_\mu^{\text{em}}(x)$ is the electromagnetic current and $V_\mu(x)$ is the vector meson current. The expression can be stated simply by noting that when the photon interacts with a hadron or is scattered by a hadron the photon behaves as if it were a combination of

vector mesons. The vector dominance model gives the following relationships:

$$\frac{d\sigma}{dt}(\gamma P \to vP) = \frac{\gamma_v^2}{\alpha\pi}\frac{d\sigma}{dt}(\gamma P \to \gamma P)$$

$$\frac{d\sigma}{dt}(\gamma P \to vP) = \frac{\alpha\pi}{\gamma_v^2}\frac{d\sigma}{dt}(vP \to vP).$$

The optical theorem, which relates the forward scattering amplitude to the total cross section can also be applied to give the relationships

$$\frac{d\sigma}{dt}(\gamma P \to vP) = \frac{\gamma_v^2}{16\pi^2\alpha}\sigma_T^2(\gamma P)(1+\beta_{\gamma N}^2)$$

$$\frac{d\sigma}{dt}(\gamma P \to vP) = \frac{\alpha\pi}{16\gamma_v^2}\sigma_T^2(vP)(1+\beta_{vN}^2)$$

when β_{vN} is the ratio of the real to imaginary part. In addition, the additive quark model gives simple relationships

$$\sigma_T(\rho_0 P) = \sigma_T(\omega P) = \tfrac{1}{2}(\sigma_T(\pi^+ P)+\sigma_T(\pi^- P))$$

$$\sigma_T(\phi P) = \sigma_T(K^+ P)+\sigma_T(K^- N)-\sigma_T(\pi^+ P).$$

All these relationships can be used to give cross sections which can be compared with experiment, and this has been one of the major aims of vector meson photoproduction.

3.1. Production of vector mesons in H_2

3.1.1. ρ meson production. The photoproduction of ρ mesons in H_2 has been carried out by counter experiments and by bubble chambers at the various electron laboratories. The counter method of detecting ρ mesons is typical of that of a Cornell group (McClellan *et al* 1969) illustrated in figure 4, where the two charged pions from the ρ decay are

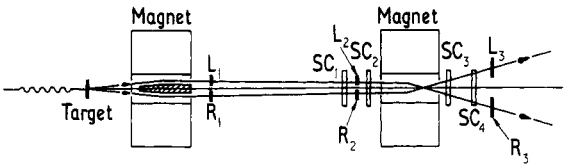

Figure 4. The di-boson spectrometer of the Cornell group for measuring forward ρ^0 photoproduction.

momentum analysed in a symmetric configuration of counters (L) and spark chambers (SC). These experiments are generally restricted to forward angles and measurement of pions produced at 90° in the ρ^0 centre of mass (CM) system. The cross section is then determined from the di-pion spectrum. However, there are several difficulties which arise in obtaining cross sections due to experimental backgrounds and the particular model required to parametrize the di-pion mass spectrum. In counter experiments particularly, the lack of knowledge of the photon energy in a bremsstrahlung beam can produce additional lower mass pion pair backgrounds, which distort the mass spectrum. As it is well established that the ρ spectrum is distorted due to an interference

mechanism between the resonant p wave $\pi^+\pi^-$ state and a nonresonant $\pi^+\pi^-$ background (Söding 1965), then an exact determination of the shape is essential to determine a cross section. In bubble chambers, the complete final state ($\pi^+\pi^-$p) is measured, and therefore the difficulties of obtaining cross sections arise due to the uncertainty of the model used to describe the physics of the interaction.

The differential cross section $d\sigma/dt$ is plotted as a function of t over a wide range of energies in figure 5 (Anderson *et al* 1970a), showing that the production mechanism is diffractive and the cross section does not change appreciably with energy. The total

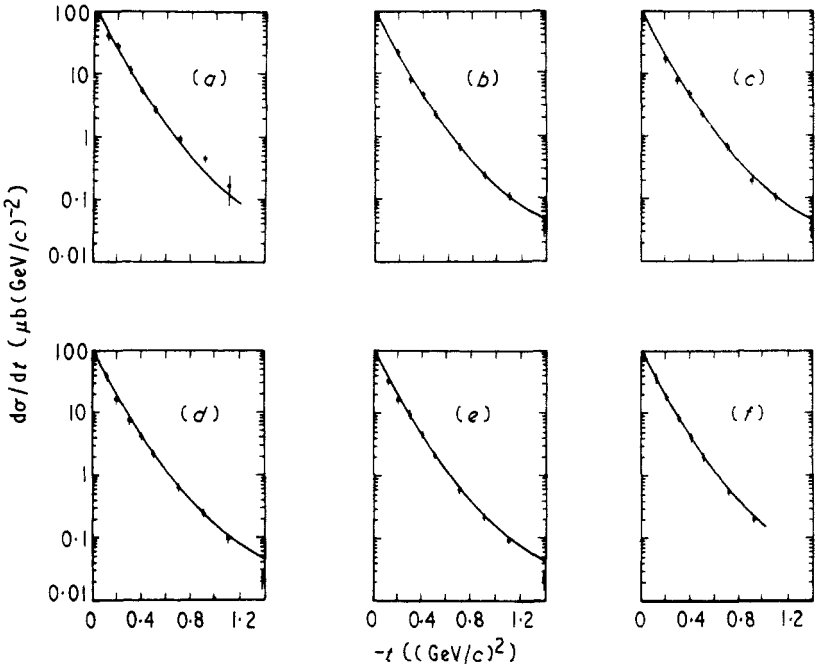

Figure 5. $d\sigma/dt$ in $\mu b\,(GeV/c)^{-2}$ against t for ρ^0 photoproduction ($\gamma + p \rightarrow \rho^0 + p$) at incident photon energies between 6 and 18 GeV measured at SLAC. Incident energies E_0 (GeV) are given by (*a*) 6·5, (*b*) 11·5, (*c*) 13·0, (*d*) 14·5, (*e*) 16, (*f*) 17·8.

cross section for ρ^0 production on hydrogen decreases slowly over this wide energy range. This is a property which is common to photoproduction in that many of the cross sections are constant and show that the 'high energy' behaviour extends down to photon energies of 3·0 GeV. The full curves in figure 5 are results obtained from πp scattering using the quark model together with vector dominance, and a value of $\gamma_\rho^2/4\pi = 0{\cdot}6$. Clearly there is remarkable similarity between the ρ meson and π meson in their interaction with the nucleon within the framework of the vector dominance model.

The forward cross section for ρ meson photoproduction is presented in figure 6, and shows that the determination varies between the different experiments. In addition, using different models to obtain cross sections can introduce a variation of up to 30%. These questions can be resolved to some extent by more precise data covering a wider pion pair mass interval and also data at lower and higher energies. However, until an

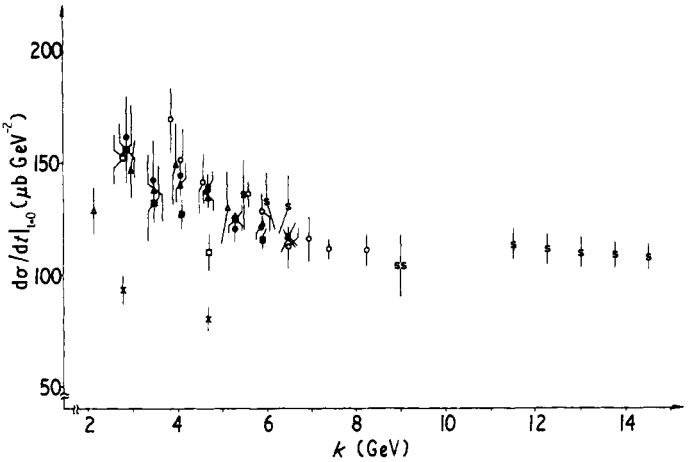

Figure 6. Summary of the data on $d\sigma/dt|_{t=0}$ for the reaction $\gamma p \rightarrow \rho^0 p$ as a function of photon energy. ● ■ ▲ DESY–MIT; ○ Cornell; s SLAC; ss SLAC; □ SLAC; × SLAC; △ DESY.

independent measurement is made of the exact shape of the ρ meson, then there will always be some difficulties in extracting cross sections from pion pair mass distributions.

3.1.2. ω meson production. Counter experiments on ω meson photoproduction are very few since the dominant 3 pion state requires more sophisticated detection compared to the simple di-pion state. In addition, counter experiments suffer from additional inelastic contributions, which are difficult to exclude unless the gamma ray energy is known. Bubble chamber measurements have been obtained at SLAC (Ballam *et al* 1970a) and DESY (ABBHHM collaboration 1968) on ω production and indicate that production due to one pion exchange (OPE) is present as well as diffractive production. The diffractive nature of ω production can be seen in figure 7, which illustrates the results of a Rochester–

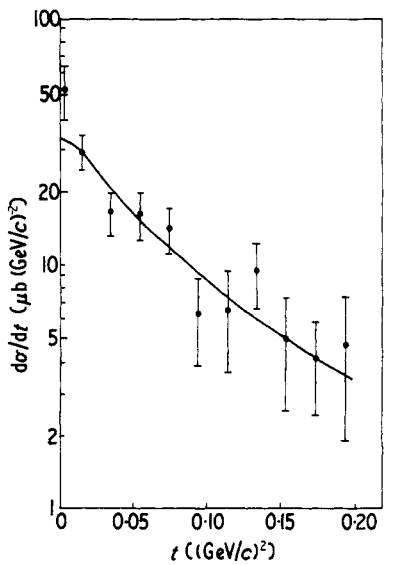

Figure 7. $d\sigma/dt$ in $\mu b\,(GeV/c)^{-2}$ against t for ω photoproduction ($\gamma + p \rightarrow \omega + p$) at 9 GeV.

Cornell group who measured ω production at 7 GeV in a counter experiment. The fit to the data uses the same t dependence as that for ρ meson production in the same energy range. The general conclusion from these experiments is that diffractive ρ production is about 9 times that for ω production, but the precise determination of $\gamma_\rho^2/\gamma_\omega^2$ from these measurements is still subject to all the uncertainties of the ρ production cross sections.

3.1.3. φ meson production. The photoproduction of φ mesons is very much less than was expected on conventional SU(3) ideas, but the quark model provides an answer since the value of $\sigma_{\phi N}$ is of the order of 15 mb, compared to a value of 27 mb for ρ and ω total cross sections at an energy of 5 GeV. Vector dominance would then give a low value for φ meson production. The φ meson decays into $K\bar{K}$ as well as 3πs and therefore counter experiments have been carried out detecting the K^+K^- decay. The results of φ meson photoproduction are presented in figure 8, when $d\sigma/dt$ is plotted against t.

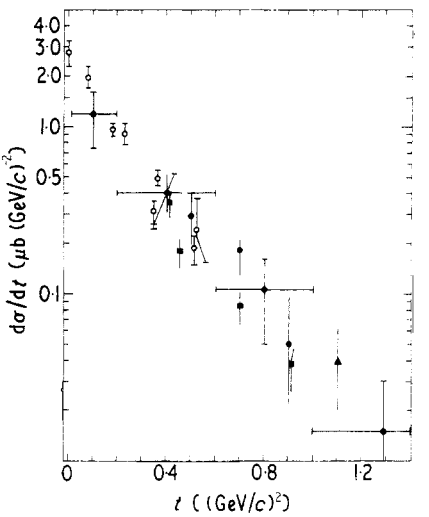

Figure 8. $d\sigma/dt$ in μb $(GeV/c)^{-2}$ against t for φ photoproduction in the energy range 2·5 to 11·5 GeV. ○ Cornell 8·5 GeV; ⊹ DESY(HBC) 2·5–5·8 GeV; ■ SLAC 11·5 GeV; ● SLAC 6·5 GeV; ▲ SLAC 6·0 GeV.

The data is independent of energy and a fit to the Cornell data (McClellan *et al* 1971a) gives

$$\frac{d\sigma}{dt} = (2{\cdot}85 \pm 0{\cdot}2)\exp\{(5{\cdot}4 \pm 0{\cdot}3)t\} \qquad (\mu b\ GeV^{-2}).$$

The φ meson is particularly interesting since it should not couple to the nucleon other than by pomeron exchange as a consequence of its strange quark components. It is evident that much more data are required over a larger s and t range before any statement on the uniqueness of the pomeron exchange mechanism to φ meson photoproduction can be made.

4. Compton scattering. The elastic scattering of photons off protons has always been **dered** as a basic experiment since the relationship between the forward scattering

amplitude and total photon cross sections serves as a check on forward dispersion relations. In addition, the relationship between this process and diffractive vector meson production provides a sensitive test of the vector dominance model. The experiments are very difficult to carry out since the cross section is small and there is a large background from π^0 production. The coplanarity between the recoiling proton and gamma ray makes the experiment possible. Two experiments have been carried out at SLAC (Anderson *et al* 1970b) and DESY (Buschhorn *et al* 1970) and the SLAC results are presented in figure 9. Here we can see that vector dominance is not working particularly at larger t values, under the assumption that the ρ, ω and ϕ vector mesons describe the photon interaction. More data are required at small t in order to provide a better comparison with the optical point, and also at larger t where nondiffractive processes should become more important for Compton scattering.

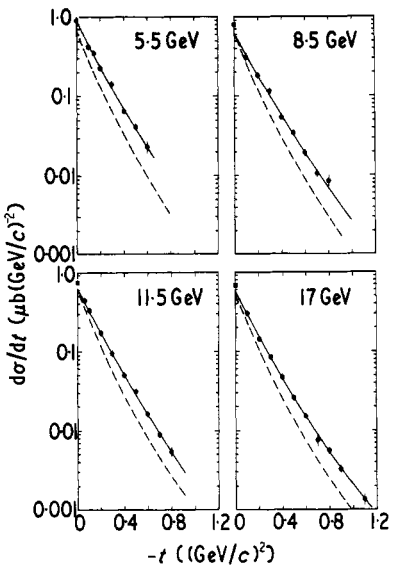

Figure 9. $d\sigma/dt$ in $\mu b\,(GeV/c)^{-2}$ against t for Compton scattering at SLAC. ● SLAC data; ■ optical point. The full curve is the least squares fit to the data and the broken curve is the vector dominance prediction.

4. Vector meson production using polarized photons

The use of linearly polarized photons is a very powerful technique to study vector meson production since the relative amount of natural parity ($P = (-1)^J, \sigma^n$) and unnatural parity ($P = -(-1)^J, \sigma^u$) exchange in the t channel can be separated as they lead to different decay angular distributions as the parity asymmetry P_σ is given by

$$P_\sigma = \frac{\sigma^n - \sigma^u}{\sigma^n + \sigma^u} = 2\rho^1_{1-1} - \rho^1_{0-0}$$

where ρ_{ik} is the ρ density matrix. Linear polarized photons of polarization P_γ can be produced at the expense of energy by coherent scattering off a diamond crystal ($P_\gamma \simeq 50\%$) and by Compton back scattering using a laser beam ($P_\gamma \simeq 95\%$). In counter experiments using the much higher intensity diamond crystal technique, the experiments

measure the yields of pion pairs (ρ meson) emitted in the plane of polarization ($\sigma_{\parallel}$) and perpendicular to it ($\sigma_{\perp}$). The asymmetry parameter Σ then determines the relative contributions from natural and unnatural parity exchange

$$\Sigma = \frac{\sigma_{\parallel} - \sigma_{\perp}}{\sigma_{\parallel} + \sigma_{\perp}} = \frac{\rho^1_{11} + \rho^1_{1-1}}{\rho^0_{11} + \rho^0_{1-1}}.$$

If natural parity exchange contributions dominate then Σ = 1, however it is important to realize that the method cannot separate the various contributions of the natural and unnatural parity exchanges.

For ρ meson production, the ratio Σ is plotted in figure 10, showing that the process is dominated by natural parity exchange, that is, pomeron exchange. The power of the polarized photon technique is illustrated in figure 11 (Ballam *et al* 1970b), where the θ

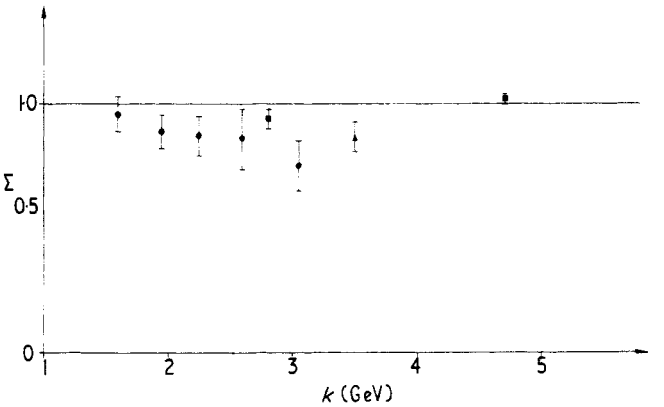

Figure 10. The polarization asymmetry parameter Σ as a function of photon energy for ρ^0 photoproduction ($\gamma + p \rightarrow \rho^0 + p$). ■ SLAC, $|t| < 1\,(\mathrm{GeV}/c)^2$; ● DESY, $|t| < 0{\cdot}4\,(\mathrm{GeV}/c)^2$; ▲ Cornell.

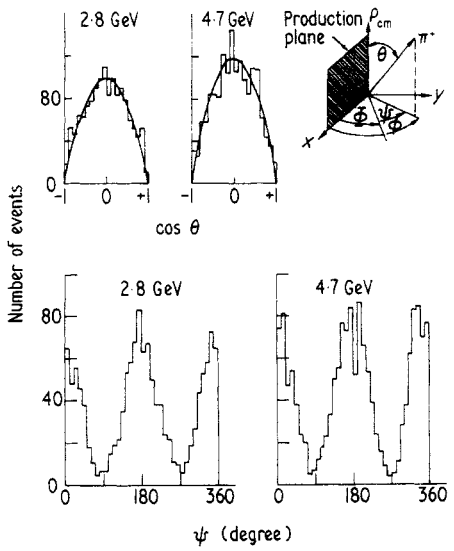

Figure 11. The decay angular distributions of the ρ^0 in the helicity frame. The distributions are proportional to $\sin^2\theta$ and $(1 + P_\gamma \cos 2\psi)$.

polar angle distribution in the helicity frame shows that the ρ conserves the helicity of the photon and the ϕ distribution indicates that natural parity exchange dominates the reaction. This has led to speculation that diffraction processes in general conserve helicity in the s channel, but at present the proof is incomplete since in the small t range of these experiments, angular momentum considerations would suggest a similar result and therefore recoil proton polarizations should also be measured.

For ω production, the results illustrated in figure 12 show that the unnatural parity exchange processes are of the same order as the natural parity processes at $E_\gamma = 4{\cdot}7$ GeV and increase towards lower energy, consistent with the S^{-1} behaviour of the one pion

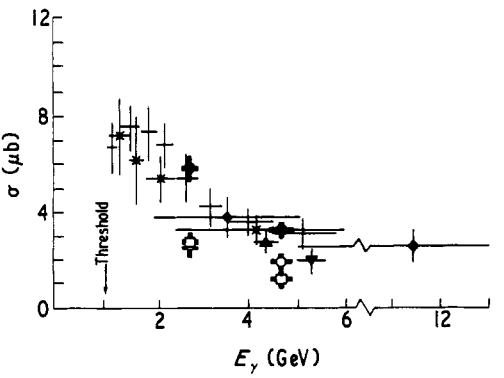

Figure 12. The total cross section for ω photoproduction ($\gamma + p \rightarrow \omega + p$) against photon energy. The contributions of natural and unnatural parity exchanges are indicated at 2·7 and 4·7 GeV.

exchange, which is expected to dominate the unnatural parity exchange contribution. The idea of using the natural parity process to determine the ratio $\gamma_\rho^2/\gamma_\omega^2$ via vector dominance is difficult since ω production could include a large amount of A_2 exchange, which is expected to be small in ρ^0 production.

Recently a new measurement of ϕ production on H_2 has been made by the Cornell Group (McClellan *et al* 1971b) using 6 GeV polarized photons. Clearly it is expected that if our previous ideas on the ϕ are correct then no unnatural parity exchanges should occur and therefore $\Sigma = 0$. However, it is found that $\Sigma = 0{\cdot}53 \pm 0{\cdot}15$ which suggests a large contribution ($\simeq 30\%$) from unnatural parity exchange contributions. It is difficult to reconcile this result with current ideas on ϕ photoproduction even allowing for inelastic contributions and more measurements are required at other energies.

5. Production of vector mesons on complex nuclei

The use of complex nuclei as a method of producing coherent vector mesons through well understood production channels has provided much more interesting physics than is generally the case when targets other than hydrogen are used. In the small t region, the sharp forward diffractive peak together with the $A^{1{\cdot}7}$ dependence indicates that coherent production is the main source of vector meson production, when the nucleus remains in the ground state. This forward beam of particles in a well defined production state can then be used to measure total cross sections for these short lived incident mesons as suggested by Drell and Trefil (1966) and illustrated in figure 13.

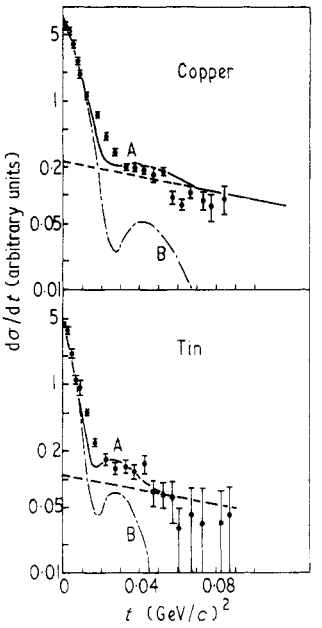

Figure 13. $d\sigma/dt$ in arbitrary units against t at 6 GeV incident photon energy. The smooth curves are the optical model predictions with (curves A) and without (curves B) an incoherent background.

The relationship between nuclear production and nucleon production is given by

$$\left.\frac{d\sigma}{dt}\right|_{t_{min}} (\gamma A - VA) = \left.\frac{d\sigma}{dt}\right|_{t_{min}} (\gamma N \to \rho N) N_{eff}^2(\sigma_{vN}, A, \beta_v, k, M_v)$$

where

$$t_{min} = -\frac{M_v^4}{4K^2}$$

and

$$N_{eff} = -2\pi \int_0^{\infty} \int_{-\infty}^{+\infty} \underbrace{b\, db\, dZ J_0(q, b)\rho(b, Z)}_{\text{nuclear size}} \underbrace{\exp\{i(-t_{min})^{1/2} Z\}}_{\text{mass dependence}} \underbrace{\exp\{-\tfrac{1}{2}\sigma_{vN}(1 - i\beta_v)\}}_{\text{meson attenuation}}.$$

Vector dominance relates the differential cross section to the total cross section by

$$\left.\frac{d\sigma}{dt}\right|_{t_{min}} (\gamma A \to VA) = \frac{\alpha}{\gamma_v^2} \frac{\sigma_{vN}^2}{16} f(\sigma_{vN}, \rho(b, Z), t_{min}).$$

Hence, the value of σ_{vN} can be obtained from the A dependence of the differential cross section, and in addition a value of γ_v^2. In general the value of σ_{vN} is consistent with quark model predictions, but the value of γ_v^2 is consistently larger than that obtained from storage ring determinations, and is dependent on the value of β_v, the ratio of real to imaginary vector meson–nucleon scattering amplitudes. The results of the various

experiments are presented in table 3, showing that the method of obtaining σ_{vN} works well, but the determination of γ_v^2 is an indication of the limitations of the technique. More precise data are required to determine $\sigma_{\omega N}$ and $\sigma_{\phi N}$ and here experiments are required which can separate out the incoherent backgrounds as for example the method of a Lancaster University Group (Atkiss *et al* 1969) working at NINA, who use monochromatic photons and spark chambers.

Table 3. Determination of σ_{vN}, ϕ_{vN} in complex nuclei

Experiment		σ_{vN} (mb)	$\gamma_v^2/4\pi$	α_{vN} (assumed)
	Energy (GeV)	ρ^0 production		
	6·1	$26{\cdot}1 \pm 0{\cdot}9$	$0{\cdot}58 \pm 0{\cdot}03$	$-0{\cdot}27$
Cornell	6·5	$30{\cdot}1 \pm 1{\cdot}5$	$0{\cdot}74 \pm 0{\cdot}05$	$-0{\cdot}27$
	8·8	$26{\cdot}8 \pm 1{\cdot}2$	$0{\cdot}68 \pm 0{\cdot}04$	$-0{\cdot}24$
DESY–MIT	6·6	$26{\cdot}7 \pm 2{\cdot}0$	$0{\cdot}57 \pm 0{\cdot}10$	$-0{\cdot}20$
Rochester	8·0	$26{\cdot}8 \pm 2{\cdot}4$	$0{\cdot}62 \pm 0{\cdot}12$	$-0{\cdot}20$
	6·0	$30{\cdot}2 \pm 3{\cdot}0$	$0{\cdot}66 \pm 0{\cdot}14$	—
SLAC	12·0	$28{\cdot}6 \pm 2{\cdot}5$	$0{\cdot}70 \pm 0{\cdot}14$	—
	18·0	$27{\cdot}8 \pm 2{\cdot}5$	$0{\cdot}71 \pm 0{\cdot}14$	—
		ω production		
Bonn–Pisa	5·5	$30{\cdot}0^{+7{\cdot}0}_{6{\cdot}0}$	$5{\cdot}8 \pm 1{\cdot}3$	$-0{\cdot}20$
Rochester	6·8	$33{\cdot}5 \pm 5{\cdot}5$	$9{\cdot}5 \pm 2{\cdot}1$	$-0{\cdot}20$
		ϕ production		
Cornell	6·2	$20{\cdot}0 \pm 3{\cdot}0$	$8{\cdot}5 \pm 0{\cdot}3$	0·0
	8·25	$12{\cdot}0 \pm 4{\cdot}0$	3·4	$-0{\cdot}35$ (fit)
DESY–MIT	5·2	$11{\cdot}3 \pm 3{\cdot}0$	$3{\cdot}7 \pm 1{\cdot}4$	$-0{\cdot}20$

6. Determination of the phase of vector meson production

The standard technique of measuring the phase of a production amplitude is to use the interference method, where the other identical final state process has a well defined production amplitude. In the case of πP scattering, this is accomplished by using Coulomb scattering at very small t. In photoproduction, the Bethe–Heitler pair production process provides a well understood real amplitude. However, it is necessary to provide the same final state electron pairs and therefore we are measuring very small cross sections via the $v \to e^+e^-$ decay channel. The processes which contribute to the lepton pair final state are indicated in figure 14 and the lepton pair mass spectrum can be written as

$$N(e^+e^-) = |A_{BH}(e^+e^-)|^2 \pm 2|A_{BH}(e^+e^-)||A_v(e^+e^-)|\exp(i\phi_v) + |A_v(e^+e^-)|^2$$

where the $\pm$ sign arises due to the fact that the virtual Compton process (A_v) behaves like a one photon process under electron positron interchange, whereas the Bethe–Heitler process (A_{BH}) behaves like a two photon process. Hence if the electron and positron are interchanged in a detection system which distinguishes between the leptons the interference term changes sign. In a symmetrical detection system where the leptons are related to each other by a parity transformation, the interference term vanishes.

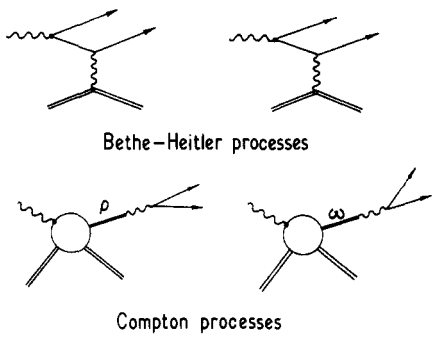

Figure 14. The processes which contribute to the electron pair mass spectrum in the region of the ρ meson in photoproduction.

A simple expression can be derived relating the measured experimental pair yields N_+ and N_- to the interference amplitude and phase (ϕ_v) by

$$\epsilon(m^2) = \frac{N^+ - N^-}{2\{\frac{1}{2}(N^+ + N^-) - N_{BH}N_{BH}\}^{1/2}} \simeq \frac{d\sigma_i}{d\sigma_v\, d\sigma_{BH}}$$

where $d\sigma_v$, $d\sigma_{BH}$ and $d\sigma_i$ are the Compton, Bethe–Heitler and interference cross sections.

The detection system required to measure these very small cross sections is illustrated by the apparatus of a Daresbury Group (Biggs *et al* 1971) in figure 15. Two independent spectrometers, each consisting of a half-quadrupole doublet and vertical deflecting magnet produce point to point focusing in the horizontal (θ) plane and line to point in the vertical (p) plane. The two spectrometer arms are therefore independent of each other in any p, θ combination.

The extent to which the interference cross section dominates the ρ meson mass region is illustrated in figure 16, when the electron pair yields for each asymmetric combination are plotted as differential cross sections against the invariant pair mass. The effect of charge conjugation, which gives rise to the $\pm$ interference term is easily seen as adding to or subtracting from the value of $d\sigma_{v+BH}$, that is, the sum of the squared amplitudes. The value obtained for the phase of ρ photoproduction off carbon by the Daresbury group is

$$\phi_{\rho A} = 16{\cdot}5° \pm 6{\cdot}2° \qquad \text{at } E_\gamma = 4\,\text{GeV}.$$

The value of the ratio of the real to imaginary part of the ρ–nucleon scattering amplitude was obtained using vector dominance to give

$$\beta_{\rho N} = -\tan\phi_{\rho N} = -0{\cdot}28 \pm 0{\cdot}12.$$

This is in good agreement with other values of $\beta_{\rho N}$ obtained from quark model, vector dominance and total photon hadron cross sections.

A similar experiment has also been carried out recently by a DESY–MIT group (Alvensleben *et al* 1970b) at 5 GeV and their results are illustrated in figure 17. The value obtained from this experiment was

$$\beta_{\rho N} = -0{\cdot}2 \pm 0{\cdot}1 \qquad \text{at } E_\gamma = 5\,\text{GeV}.$$

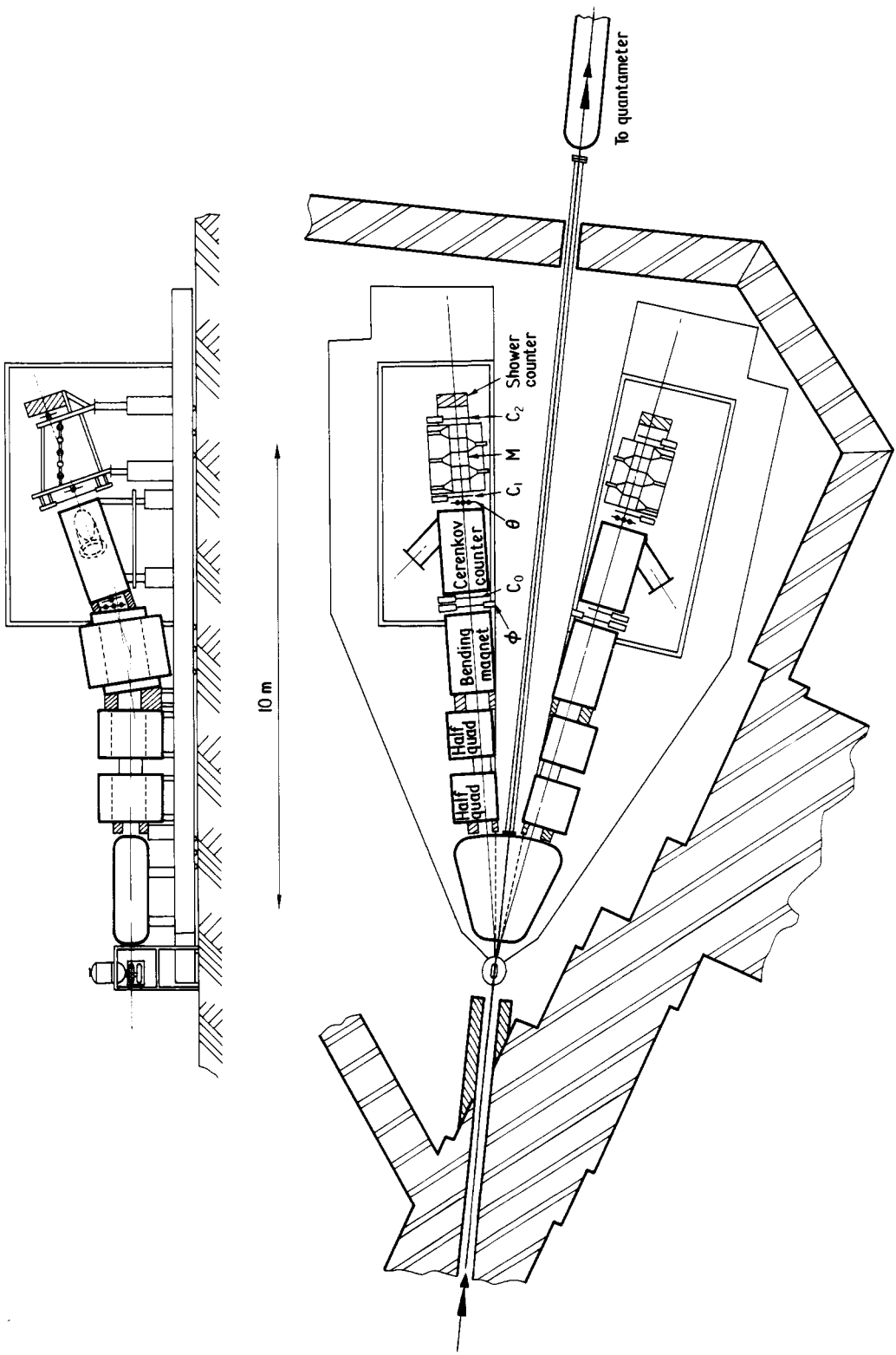

Figure 15. The Daresbury lepton pair spectrometer consisting of two independent identical spectrometers.

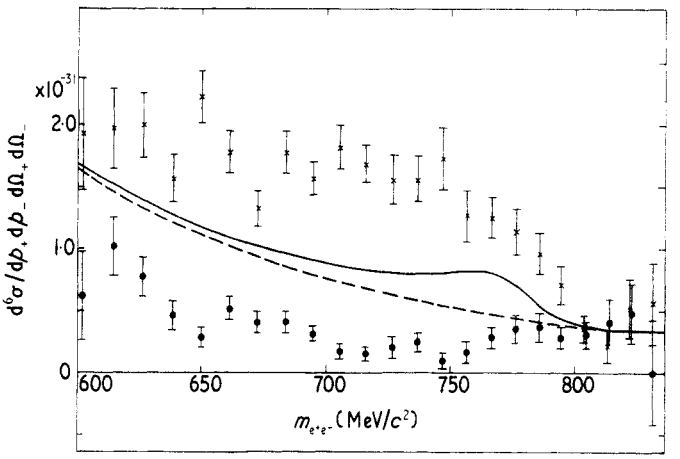

Figure 16. The differential cross section for the $N^{\pm}$ yields (units of $cm^2\,(GeV/c)^2\,sr^{-2}$/nucleon eq) as a function of invariant mass. The broken curve is the theoretical BH cross section and the full curve is the sum of the BH and fitted Compton cross sections. The full circles and crosses are data for the N^- and N^+ yields respectively.

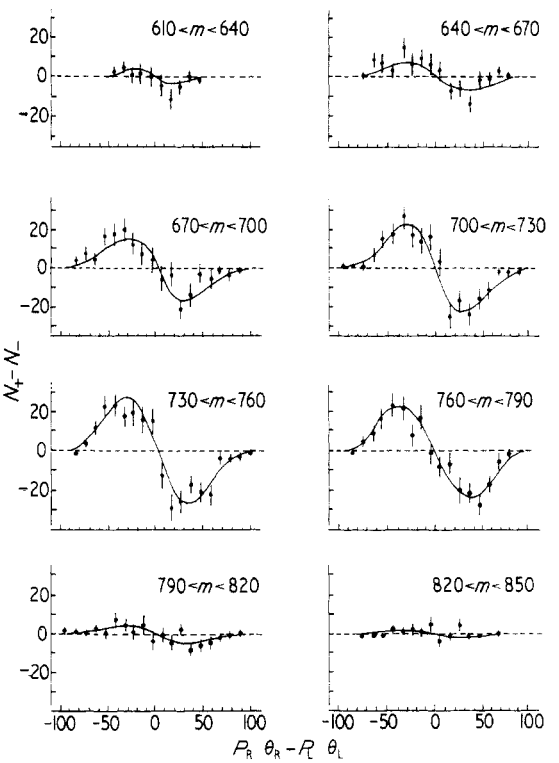

Figure 17. The measured asymmetric events $N_+ - N_-$ as a function $(P\theta)_L - (P\theta)_R$ for each mass bin of 30 MeV/c^2.

6.1. ω production phase

The determination of the phase of the ω meson production can also be measured in principle by the same method as that used for ρ meson production. However, the situation is complicated by the fact that the ω meson lies within the ρ mass region and since both mesons can decay into lepton pairs, it is possible to have interference between the ρ and ω virtual Compton amplitudes as well as with the Bethe–Heitler amplitudes.

The spectrum of lepton pair final state events can be simplified by performing a symmetric experiment where the interference between the Compton and Bethe–Heitler amplitudes vanishes and only the ρ–ω interference term remains in the Compton amplitude. In this way the ω production phase is measured with respect to that of the ρ meson. The effect of ω–ρ interference is illustrated in figure 18, where the Compton lepton pair

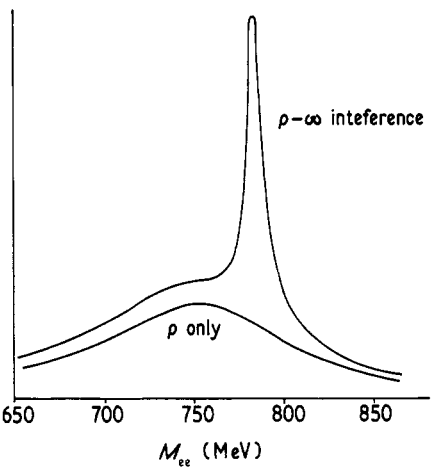

Figure 18. The theoretical lepton pair mass spectrum in the ρ^0 region showing the effect of ρ–ω interference assuming $\gamma_\omega^2/\gamma_\rho^2 = 9$.

spectrum is plotted against the lepton pair invariant mass. If the two production amplitudes are in phase, that is $\phi_{\omega\rho} = 0$, as might be expected on a simple diffraction model, then a large interference peak is observed at the ω mass even though the cross section for ω production is only about $\frac{1}{9}$ that of ρ meson production. It is interesting to note that previous experiments even if they did not have a narrow mass resolution ($\simeq \pm 5$ MeV) would still have observed a much larger branching ratio for $\rho \to e^+e^-$ than storage ring measurements, where the electron pairs occur in the initial state.

The Compton lepton pair spectrum as measured in a Daresbury experiment (Biggs *et al* 1970a) is presented in figure 19, and shows clear evidence that ρ–ω interference does occur. The result of the experiment gives

$$\phi_{\rho\omega}^{ee} = 100^\circ {}^{+38^\circ}_{-30^\circ} \qquad \text{at } E_\gamma = 3{\cdot}6 \text{ GeV}.$$

This result is somewhat surprising since the experiment was performed using a carbon target and only coherent ω production can interfere with coherent ρ production. However the value obtained in this experiment for the ratio $\gamma_\rho^2/\gamma_\omega^2$ which is phase dependent was $7{\cdot}0^{+2{\cdot}1}_{-1{\cdot}5}$, which is in good agreement with the storage ring determination. The results

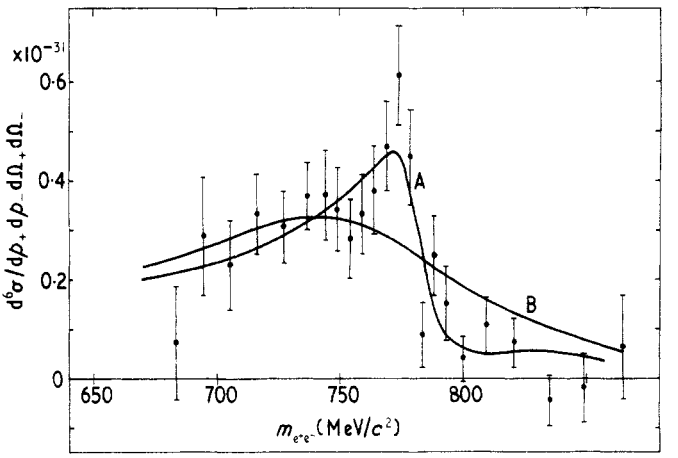

Figure 19. The differential Compton cross section (units of cm^2 $(GeV/c)^2$ sr^{-2}/nucleon eq) against lepton pair invariant mass. The two curves are the best fits to the data, A with and B without interference.

of an experiment carried out at DESY (Alvensleben *et al* 1970a) are presented in figure 20, and that experiment gives

$$\phi_{\rho\omega}^{ee} = 41° \pm 20° \qquad \text{at } E_\gamma = 5{\cdot}0\,\text{GeV}.$$

This experiment gives a lower value of $\phi_{\rho\omega}$, but the two experiments are very similar when comparing their mass spectra. A more precise experiment ($\pm 5°$) would require

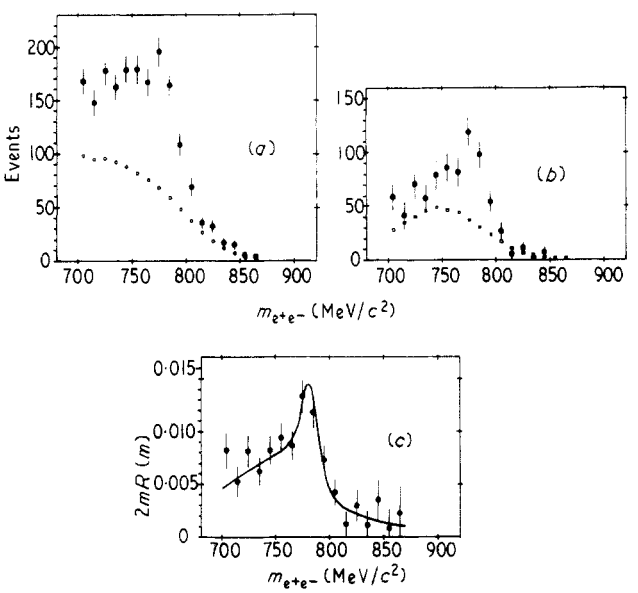

Figure 20. The lepton pair spectrum against lepton pair invariant mass showing (*a*) complete spectrum including BH events (ϕ data, 2841 events; ● BH, 1618 events), (*b*) Compton spectrum only (ϕ data, BH removed; □ ρ contribution) and (*c*) unfolded spectrum (ϕ data; —theory).

an improvement in statistics by a factor of ten over existing experiments with an absolute mass calibration of 1 MeV/c.

6.2. ϕ production phase

A measurement of the phase of ϕ photoproduction has not yet been made, but in principle could be done by a Bethe–Heitler interference method. However, the question of whether the phase of ϕ photoproduction is zero or in accord with quark model predictions of about 20° would be very difficult to determine since the 4 MeV width of the ϕ meson is much narrower than present detection equipment (FWHM = 10 MeV).

7. Other applications of interference methods

The method of interference just outlined in electron pair decays can also be used to look for rare decays such as the $\omega \to 2\pi$ which is a G parity violating decay of the ω meson. As the ρ meson decays strongly into two pions and we know from the electron pair results that interference does occur, then it should be possible to produce an effect on the overall pion pair mass spectrum.

The pion pair spectrum is given by

$$S(\pi^+\pi^-) \simeq \left(\frac{1}{m^2 - m_\rho^2 + im_\rho\Gamma_\rho} + \frac{\exp(i\alpha_{2\pi})}{m^2 - m_\omega^2 + im_\omega\Gamma_\omega}\right)^2$$

$$\alpha_{2\pi} = \phi_N + \phi$$

where $\alpha_{2\pi}$ is the relative phase of the ρ and ω, 2π final states, ϕ_N is the relative phase of the hadronic amplitudes and ϕ is the phase due to ρ–ω mixing. The overall effect of changing α is to produce a peak ($\alpha = 0$), dip ($\alpha = 180$) or wiggle in the spectrum around the ω mass.

The results of a Daresbury experiment (Biggs *et al* 1970b) are presented in figure 21, where clear evidence is seen of an interference effect in the region of ω mass. The results of this experiment give

$$\alpha_{\pi\pi} = 104{\cdot}0° \pm 5{\cdot}1° \qquad \mathrm{BR}\left(\frac{\omega \to 2\pi}{\omega \to \mathrm{all}}\right) = 0{\cdot}80\,\%^{+0{\cdot}28}_{-0{\cdot}22}\,\% \qquad m_\omega = 783 \pm 1{\cdot}6\ \mathrm{MeV}.$$

The value of the phase ϕ can be considered in the following manner. If the value of $\phi_N = 0$, that is both ρ and ω production proceed diffractively, then $\alpha_{2\pi} = 104° \pm 5{\cdot}1°$, which is in excellent agreement with the value of 110° which has been predicted by several authors (Kroll *et al* 1966 and Sachs and Willemsen 1970) based on theoretical models.

However, if the value of $\alpha^{ee}_{\rho\omega} = 100°^{+38°}_{-30°}$ is used as measured in the electron pair experiment, the value of $\alpha_{2\pi}$ is reduced to approximately $\phi = 15°$, which is in disagreement with theory. However, this value of α_{ee} is supported by a recent experiment (Biggs *et al* 1971) which was carried out under an asymmetric configuration and gave a value of $\alpha^{ee}_{\rho\omega} = 118°^{+13°}_{-22°}$. It is difficult to reconcile the results of the electron pair experiment with that of the pion pair experiment, if we believe that the value of $\alpha^{\pi\pi}$ should be around 100°. The value of $\alpha^{\pi\pi}$ has also been obtained from ρ–ω interference experiments using electron–positron colliding beams. The value obtained in this experiment

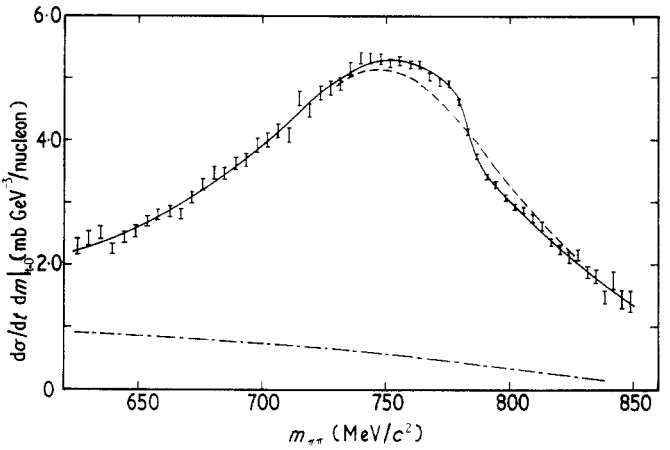

Figure 21. Differential cross section against pion pair invariant mass. The full curve is the best fit to the data, the chain curve is the same fit without ω interference. Total number of events is about 200 000.

(Augustin *et al* 1969b) which suffers from a lack of statistics is $164° \pm 28°$, but a recent measurement (Perez-y-Jorba, private communication) gives a value of $\alpha^{\pi\pi}$ about 90°.

The possibility of looking at the $\phi \to 2\pi$ decay by ρ–φ interference is possible but very difficult since the mass difference in the Breit–Wigner denominator of the interference amplitude is approximately 240 MeV as compared with only about 20 MeV in the case of ρ–ω interference.

8. Searches for high mass vector mesons

Various experiments have been carried out by various groups to look for high mass vector mesons. These experiments fall into two classes. In one, the process

$$\gamma + C \to e^+ + e + C$$

is studied where the lepton pair spectrum is plotted against lepton pair mass. These experiments have the advantage that the background process, that is Bethe–Heitler, is well understood and therefore any excess in the lepton pair spectrum over Bethe–Heitler is evidence of a 1^- vector meson which couples to the photon. The main disadvantage is that the $v \to \gamma \to e^+e^-$ coupling produces small cross sections.

In the other type of experiment the process $\gamma + C \to C + \pi^+ + \pi^-$ is studied and the pion pair invariant mass spectrum is recorded and investigated for possible pion pair resonances. This experiment has the advantage of good statistical accuracy but suffers from a lack of knowledge of the nonresonant background and even if a bump is seen, it may not be due to a 1^- vector meson. However, at present there is no evidence to suggest that any high mass vector mesons have been found in the mass region up to 2 GeV, and therefore if they do exist, then their value of $\gamma_v^2/4\pi$, which is inversely proportional to the photon–vector meson coupling must be large.

In conclusion, the study of vector mesons so far has produced some very interesting new physics ideas and results. If we look at the total data, there are still many regions

which have not yet been investigated and there will be many new questions to be answered when much better quality data become available from polarized photons and polarized targets as well as going to higher energies.

References

ABBHHM collaboration 1968 *Phys. Rev.* **175** 1669–96
Alvensleben H *et al* 1970a *Phys. Rev. Lett.* **25** 1373–6
Alvensleben H *et al* 1970b *Phys. Rev. Lett.* **25** 1377–80
Anderson R L *et al* 1970a *Phys. Rev.* D **1** 27–47
Anderson R L *et al* 1970b *Phys. Rev. Lett.* **25** 1218–22
Atkiss M *et al* 1969 *Daresbury proposal DNPL/SCP* 48
Augustin J E *et al* 1969a *Phys. Lett.* **28B** 508–12
Augustin J E *et al* 1969b *Lett. Nuovo Cim.* **12** 214
Ballam J *et al* 1970a *Phys. Rev. Lett.* **24** 1364–8
Ballam J *et al* 1970b *Phys. Rev. Lett.* **24** 960–3
Biggs P J *et al* 1970a *Phys. Rev. Lett.* **24** 1197–200
Biggs P J *et al* 1970b *Phys. Rev. Lett.* **24** 1201–5
Biggs P J *et al* 1971 *Phys. Rev. Lett.* **27** 1157–60
Buschhorn G *et al* 1970 *Phys. Lett.* **33B** 241–4
Drell S D and Trefil J S 1966 *Phys. Rev. Lett.* **16** 552–5
Kroll N M, Lee T D and Sumino B 1967 *Phys. Rev.* **157** 1376–99
McClellan G *et al* 1969 *Phys. Rev. Lett.* **22** 374–7
McClellan G *et al* 1971a *Phys. Rev. Lett.* **26** 1597–9
McClellan G *et al* 1971b *Cornell preprint CLNS*-154
Nambu Y 1957 *Phys. Rev.* **106** 1366–7
Sachs R G and Willemsen J F 1970 *Phys. Rev.* D **2** 133–6
Söding P 1965 *Phys. Lett.* **19** 702–4